Supporting Information

Antoniades et al. 10.1073/pnas.1106378108

SI Materials and Methods

Subsampling of Cores for Analysis. The two longest cores obtained from Disraeli Fiord were selected for analysis. These cores, 38 and 47 cm in length (hereafter called core 3 and core 4, respectively), were sealed and transported whole to Université Laval. Core 3 was taken in 55 m of water, and core 4 was taken at 69-m water depth. The sediment–water interface was captured intact in core 3, as indicated by the intact invertebrate tubes on the sediment surface upon core retrieval (Fig. S2). Both cores were composed of massive silty clay with diffuse color banding. Particle size qualitatively varied little throughout the core, and there were no evident coarse layers. X-radiographs (Fig. S1) confirmed the lack of lithological change and showed that the observed geochemical changes did not correspond to any observable changes in sediment lithology. Ice-rafted debris was also rare in the cores (Fig. S1). Al:Ti ratios (Fig. S1), used as an indicator of sediment provenance (1), showed limited variation in both sediment sequences, indicating that changing source regions could not be invoked as the cause of the observed geochemical shifts.

Both cores were split lengthwise, and subsamples were taken for preparation using a number of techniques. One half of each core was reserved for pigment analysis. Subsamples were taken every 0.25 cm; however, preliminary preparations indicated that pigment concentrations were too low for quantification at this resolution. Intervals were therefore combined, and lyophilized samples of ~3 g (dry weight) were extracted with 10–15 mL of 100% acetone. The extracts were subsequently evaporated to dryness under a stream of argon and resuspended in 1 mL of acetone for injection into the HPLC. Samples for pigment analysis were taken along the entire length of core 3 as well as over the top 12 cm and at the base of core 4. Organic matter analysis was also performed with material from these same intervals using loss on ignition (2); these values were used to correct pigment concentrations to organic matter concentration.

Magnetic susceptibility and paleomagnetic measurements were performed along the entire length of both cores, whereas X-ray fluorescence (XRF) measurements were taken every 200 μm with the Itrax core scanner over the upper 28 cm of core 3 and all of core 4. The records of total carbon (organic and inorganic), carbon isotope composition of organic carbon ($\delta^{13}C_{ORG}$), and foraminifera represent samples taken from both cores. Samples from core 3 were taken from sediments representing recent deposition to ~1,400 calibrated (cal) ka BP, whereas those from core 4 were taken from ~1,100 cal ka BP to the base of the record, with overlap preserved in all cases to permit verification of consistency between the core sections.

Age–Depth Model Construction. The age–depth model was constructed by using Markov chain Monte Carlo Bayesian methods with the program WinBacon (3). The model was constructed based on seven accelerator mass spectrometry (AMS) dates of hand-picked foraminiferal ^{14}C (Table S1) and four key inflection points in the paleomagnetic record (Fig. 2). Radiocarbon dates were calibrated with the Marine09 dataset (4), a local ΔR of 335 ± 85 y was applied to all samples (5), and an additional variable carbon reservoir (Table S1) was applied to samples within epishelf stages assuming a fixed carbon pool because of isolation by the strong perennial ice cover, as observed in proglacial lakes (6, 7). The age of epishelf stages was calculated from paleomagnetic data, and the carbon reservoir was assumed to be fixed at this point. The number of years elapsed between the date of epishelf formation and the ^{14}C age was then added to the local ΔR for each radiocarbon date (Table S1). The carbon reservoir was assumed to have reequilibrated with the atmosphere during break-up events. The model was constructed in 4-cm sections, with prior probabilities set as follows: mean accumulation, 250 y cm^{-1}; accumulation shape, 4; memory mean, 0.6; and memory strength, 120. Models were based on runs of 1,440,000 iterations of which every 60th iteration was retained; the process was repeated several times to ensure stability and convergence of the results. The maximum a posteriori model (i.e., best fit; Table S2) had a mean 95% confidence interval of ± 331 years and a log of the posterior of −49.55. Ages beyond the lowest model section were calculated by linear extension of the sedimentation rate.

Radiocarbon samples between 2.25 and 8.25 cm with age reversals were excluded from the model (Table S2). We hypothesize that ancient carbon flushed from the catchment during the reformation of the epishelf lake may have produced these inflated ^{14}C ages. Two independent lines of evidence allowed us to dismiss the possibility of sediment mixing in this section of the core. First, essentially all physical and geochemical parameters in this interval were incongruent with those of lower sediments returning coeval ^{14}C ages; moreover, the consistency of paleomagnetic trends between Disraeli Fiord and regional records (Fig. 2) reinforced that mixing had not occurred. A second ^{14}C age reversal at 30.4 cm likely resulted from mollusc fragments in the sample that were either reworked or returned artificially old ^{14}C ages because of their incorporation of ancient carbon from bedrock, as occurs with numerous deposit-feeding Arctic molluscs (5). Given the absence of foraminifera in the lower section of the core, despite the attendant concerns, we attempted to date the core's base by using bulk sediment. This ^{14}C age suggested that the core bottom was aged 43.5 cal ka BP (Table S1). We are reluctant to accept such an age given its $\delta^{13}C$ value that approaches those of carbonate rocks and the potential in the region for ancient carbon contamination (8), and therefore we excluded it from the age–depth model, instead giving precedence to an extrapolated age based on the sedimentation rate derived from paleomagnetic results and numerous microfossil ^{14}C ages.

1. Martinez NC, et al. (2010) Local and regional geochemical signatures of surface sediments from the Cariaco Basin and Orinoco Delta, Venezuela. *Geology* 38:159–162.
2. Dean WE (1974) Determination of carbonate and organic matter in calcareous sediments and sedimentary rocks by loss on ignition: Comparison with other methods. *J Sediment Petrol* 44:242–248.
3. Blaauw M, Christen AJ (2011) Flexible paleoclimate age-depth models using an autoregressive gamma process. *Bayesian Anal* 6:457–474.
4. Reimer PJ, et al. (2009) Intcal9 and Marine09 radiocarbon age calibration curves, 0–50,000 years ka BP. *Radiocarbon* 51:1111–1150.
5. Coulthard RD, Furze MFA, Pienkowski AJ, Nixon FC, England JH (2010) New marine ΔR values for Arctic Canada. *Quat Geochronol* 5:419–434.
6. Hall BL, Henderson GM (2001) Use of uranium-thorium dating to determine past ^{14}C reservoir effects in lakes: Examples from Antarctica. *Earth Planet Sci Lett* 193:565–577.
7. Hendy CH, Hall BL (2006) The radiocarbon reservoir effect in proglacial lakes: Examples from Antarctica. *Earth Planet Sci Lett* 241:413–421.
8. Retelle M, Bradley RS, Stuckenrath R (1989) Relative sea level chronology determined from raised marine sediments and coastal isolation basins, northeastern Ellesmere Island, Arctic Canada. *Arct Alp Res* 21:113–125.

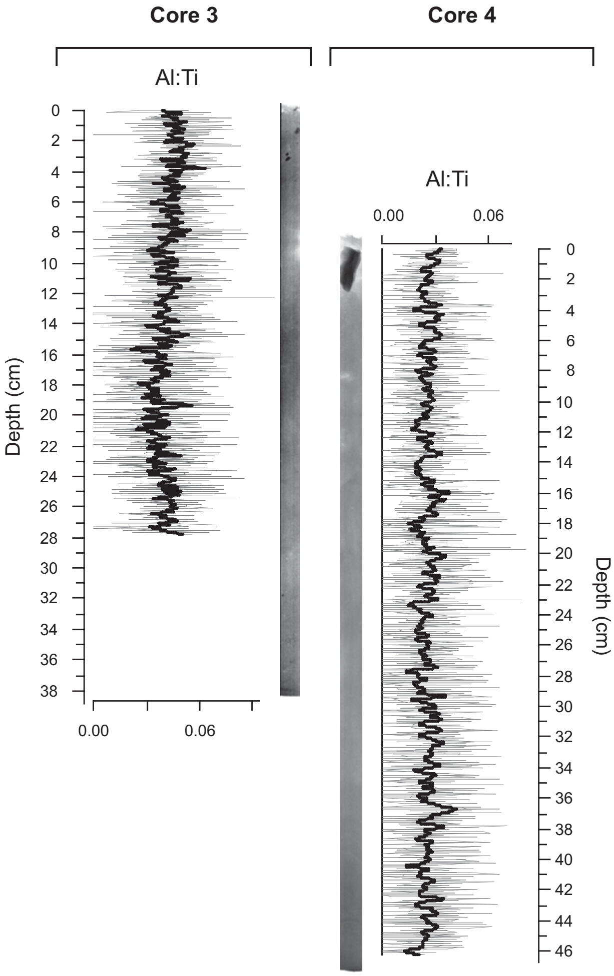

Fig. S1. Al:Ti XRF ratios and X-radiographs for the upper (core 3) and lower (core 4) core sections analyzed from Disraeli Fiord.

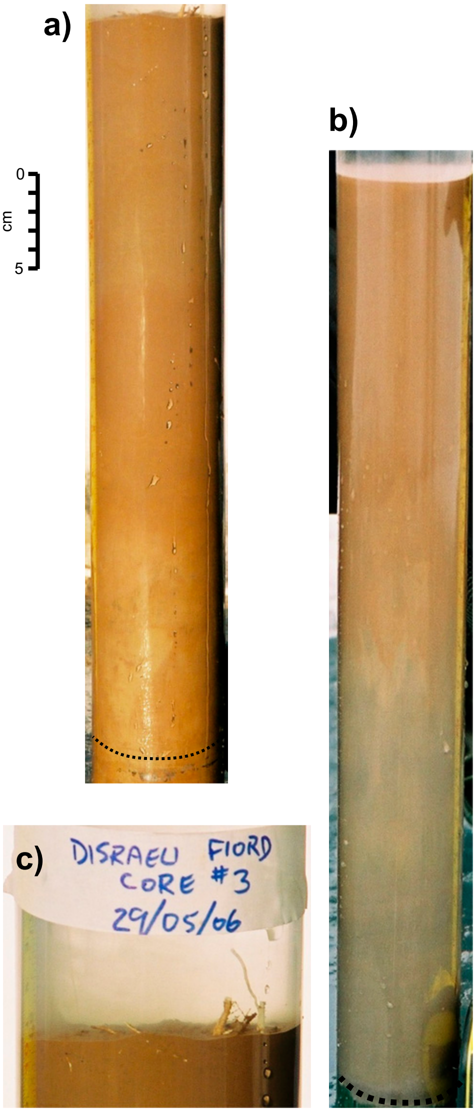

Fig. S2. Photographs of the upper (*A*) and lower (*B*) core sections analyzed from Disraeli Fiord and the sediment–water interface (*C*) of the upper core section showing intact invertebrate tubes.

Table S1. Radiocarbon dates from Disraeli Fiord sediments

Midpoint, cm	Material	cal ka BP	Radiocarbon age	2σ range	Δ*R*	δ^{13}C, ‰	Sample ID
11.25	F	1,440	2,805 ± 15	560–2,310	998 ± 417	0.3	UCIAMS-66268
11.57	F	2,200	3,450 ± 15	1,300–3,100	932 ± 384	2.5	UCIAMS-66270
13.48	F	2,710	3,485 ± 20	2,140–3,280	542 ± 229	−2.5	UCIAMS-47799
18.25	F	3,070	3,685 ± 20	2,770–3,380	425 ± 130	0.4	UCIAMS-47794
22.05	F	4,170	4,455 ± 20	3,930–4,410	335 ± 85	−1.5	UCIAMS-47798
24.25	F	7,310	7,120 ± 20	7,140–7,470	335 ± 85	−1.6	UCIAMS-47795
34.25	F	8,120	7,985 ± 15	7,940–8,300	335 ± 85	1.2	UCIAMS-66267
--------	--------	--------	--------	--------	--------	--------	--------
2.25	F	4,630	5,555 ± 20	3,530–5,730	1,057 ± 446	3.9	UCIAMS-66265
5.25	F	5,940	5,990 ± 15	5,630–6,250	444 ± 140	2.8	UCIAMS-66269
8.25	MF, CH, F	3,530	3,940 ± 40	3,290–3,760	335 ± 85	−4.2	Beta-249659
30.41	MF, F	8,690	8,495 ± 20	8,440–8,940	335 ± 85	4.9	UCIAMS-66266
52.25	Sediment	43,500	39,400 ± 1,000	42,000–45,000	335 ± 85	−2.9	UCIAMS-35971

^{14}C dates above the dashed line were used in the Bayesian age–depth model (*SI Materials and Methods*). CH, chitin; F, foraminifera; MF, mollusc fragments; UCIAMS, University of California, Irvine Accelerator Mass Spectrometry.

Table S2. Maximum a posteriori age–depth model with 95% confidence intervals (CI)

Depth, cm	Maximum a posteriori, cal ka BP	95% CI minimum	95% CI maximum
0	−66.3	−813	−13
1	−13.9	−559	56
2	38.5	−326	149
3	90.9	−117	248
4	143.3	58	378
5	294.2	176	561
6	445.1	274	779
7	595.9	351	1,001
8	746.8	430	1,250
9	933.0	683	1,398
10	1,119.3	896	1,621
11	1,305.5	1,077	1,792
12	1,491.8	1,226	2,031
13	1,885.2	1,602	2,277
14	2,278.7	1,914	2,549
15	2,672.2	2,173	2,898
16	3,065.6	2,361	3,276
17	3,191.6	2,610	3,370
18	3,317.5	2,842	3,477
19	3,443.5	3,029	3,604
20	3,569.4	3,188	3,763
21	3,816.5	3,509	3,974
22	4,063.6	3,788	4,218
23	4,310.6	4,027	4,487
24	4,557.7	4,221	4,786
25	4,865.1	4,571	5,071
26	5,172.5	4,834	5,424
27	5,479.9	5,007	5,827
28	5,787.3	5,179	6,254
29	6,047.3	5,571	6,416
30	6,307.2	5,953	6,633
31	6,567.2	6,237	6,852
32	6,827.2	6,456	7,216
33	7,189.7	6,851	7,476
34	7,552.1	7,190	7,890
35	7,914.6	7,477	8,347
36	8,277.1	7,740	8,815